Simulating different modes of current transfer to thermionic cathodes in a wide range of conditions

2009 J. Phys. D: Appl. Phys. 42 145205

(http://iopscience.iop.org/0022-3727/42/14/145205)

IOP PUBLISHING JOURNAL OF PHYSICS D: APPLIED PHYSICS

J. Phys. D: Appl. Phys. **42** (2009) 145205 (17pp) doi:10.1088/0022-3727/42/14/145205

Simulating different modes of current transfer to thermionic cathodes in a wide range of conditions

M S Benilov, M D Cunha and M J Faria

Departamento de Física, Universidade da Madeira, Largo do Município, 9000 Funchal, Portugal

Received 27 April 2009, in final form 28 May 2009
Published 1 July 2009
Online at stacks.iop.org/JPhysD/42/145205

Abstract

Changes in the pattern of steady-state modes of current transfer to thermionic cathodes induced by variations of the cathode geometry and temperature of the cooling fluid are studied numerically. For some combinations of control parameters, only one stable mode in a wide current range exists, which combines features of spot and diffuse modes. This mode, when attached to an elongated protrusion on the cathode surface, may be identified with the so-called super spot mode observed in experiments on low-current arcs. There is also reasonable agreement between the modelling and the experiment on cathodes of high-current arcs operating in the diffuse mode. The conclusions on existence under certain conditions of only one stable mode in a wide current range and of a minimum of the dependence of the temperature of the hottest point of the cathode on the arc current, manifested by this mode, may have industrial importance and admit a straightforward experimental verification.

(Some figures in this article are in colour only in the electronic version)

1. Introduction

Observations of different modes of current transfer from high-pressure arc plasmas to thermionic cathodes were reported long ago both for conditions of low-current arcs [1] and arcs with the current of a few hundred amperes [2]. Such observations have also been reported by many subsequent authors; see, e.g. [3–8] and also references and discussion in [9]. A variety of modes were observed, the most frequent being the so-called diffuse mode and a constricted, or spot, mode.

Processes governing current transfer from high-pressure arc plasmas to thermionic cathodes are many and of different nature and occur on strongly different time scales. Processes governing distributions of the ions, electrons and the electric field in the near-cathode plasma are the fastest. The relevant time scale is represented by the time of motion of the ions across the near-cathode layer where the energy flux to the cathode is generated. This time is comparable to the ionization time and, if estimated with the use of characteristic parameters of the near-cathode region of the atmospheric-pressure argon arc taken from [10], is of the order of 1 μs or lower.

Formation of diffuse and spot modes of current transfer, as well as switching between the modes, is governed by the process of conduction of heat in the body of the cathode. Since the temperature distribution inside the cathode is characterized by a variety of length scales, this process comprises several phases characterized by different time scales. The smallest and, respectively, biggest time scales are represented by the times of diffusion of heat over distances of the order of the radius of the cathode spot and, respectively, of the order of the cathode height. Taking 10^{-5} m^2 s^{-1} as a typical value of thermal diffusivity of electrode materials and assuming 50 μm as a lower estimate of the radius of the cathode spot and 10 mm as a characteristic height of the cathode, one finds that the time scales of heat conduction in the cathode body are comprised between 0.25 ms and 10 s.

It happens frequently that cathodes of high-pressure arc discharges change their shape due to melting and/or evaporation of the cathode material with subsequent return of a part of the evaporated metal to the cathode in the form of either neutral atoms (condensation of the vapour) or ions (the so-called recycling). These changes usually take from several minutes to several hours (e.g. sections 3.2 and 3.4 of [6] and section 2 of [7]).

Thus, heat propagates in the cathode body much slower than processes in the near-cathode plasma occur, but much

faster than the cathode changes its shape. It follows that, while treating the formation of diffuse and spot modes of current transfer and switching between the modes, one may assume that variations of distributions of the ions, electrons and the electric field in the near-cathode plasma, caused by variations of the potential and the distribution of temperature of the cathode surface, occur instantaneously, while variations of the cathode shape are frozen. A theoretical approach to description of diffuse and spot modes on thermionic cathodes which is developed along these lines and makes use of the thinness of a near-cathode plasma layer where the energy flux to the cathode surface is generated is frequently termed the model of nonlinear surface heating.

The model of nonlinear surface heating does not account for the effect of convective motion of the gas over the plasma–cathode interaction, on the grounds that the normal component of the gas velocity can hardly be sufficiently high in the above mentioned very thin near-cathode plasma layer where the energy flux to the cathode surface is generated. It is difficult to estimate the effect of convective motion of the gas theoretically, since the distribution of the gas velocity in the immediate vicinity of the cathode surface is unknown. The experiment seems to indicate that a convective motion of the gas is necessary for the formation of the so-called blue-core mode [11], which can occur on cathodes of low-current free-burning arcs, especially on those made of thoriated tungsten. However, there are no indications that a convective motion plays a role in the formation of the diffuse or spot modes. (It is interesting to note that the situation is different as far as modes of anode attachment are concerned: it is believed [12] that in the diffuse mode the power is supplied to the anode by a plasma flow from the bulk.) Therefore, the model of nonlinear surface heating represents an adequate tool for investigation of the diffuse and spot modes.

The model of nonlinear surface heating was proposed long ago [13]; however, its power has been universally appreciated only during the last decade; see review [9] and references therein. The most important feature of this model is the existence, under the same conditions, of multiple solutions describing the diffuse mode of current transfer and different spot modes. This feature has made a self-consistent modelling of the diffuse and spot modes on cathodes of a given shape a matter of routine. One can mention, as an example, a free Internet tool [14] for simulation of diffuse and axially symmetric spot modes on cylindrical cathodes in a wide range of arc currents, plasma compositions and cathode materials and dimensions, which also serves as a tutorial on finding multiple solutions describing diffuse and spot modes.

A pattern of different modes of current transfer studied up to now comprises a diffuse mode that exists at all currents and different spot modes that exist at currents low enough. This pattern has been established theoretically [15] with the use of ideas from the theory of self-organization in nonlinear dissipative systems and was confirmed by the numerical modelling of cylindrical cathodes with the flat front surface [16, 17]. Also fit into this pattern results of numerical modelling of cathodes with a rounded edge of the front surface [9, 18, 19] and cathodes with a hemispherical front surface [18, 20], except that the spot modes in [18, 20] were found not in the whole region of their existence. Stability has been studied only for cylindrical cathodes with the flat front surface [21, 22] and it was found that the diffuse mode is stable at all currents of interest if the cathode is thin enough and is unstable at low currents otherwise; the high- and low-voltage branches of the mode with a spot at the edge of the front surface are stable and, respectively, unstable; all the other spot modes are unstable, including axially symmetric spot modes.

However, the results of the recent numerical modelling [23] do not fit into the above-described pattern. This modelling was motivated by the experiments [6, 24] (similar experiments were also reported in [25]) and dealt with a cylindrical cathode with a hemispherical tip and a protrusion at the top of the tip. Two axially symmetric modes have been found in this modelling. One of the modes exists only at low currents and comprises two branches separated by a turning point, one of these branches being stable and another unstable. The stable branch is associated with thermal regimes of the cathode which are characteristic of the diffuse mode and there seems to be a poorly pronounced spot in thermal regimes associated with the unstable branch. The other mode exists at all currents, is Z-shaped, and manifests a smooth transition from thermal regimes characteristic of the spot mode (at low currents) to regimes characteristic of the diffuse mode (at high currents). This mode is stable except at the 'retrograde' section of the Z-shape. This mode was also found in the numerical modelling of current transfer to cylindrical cathodes with a blunt conical tip [26], which are usually employed in plasma torches for plasma spraying, cutting, welding, metal purification, extractive metallurgy, powder synthesis, etc.

The above-cited results indicate that more than one pattern of current transfer to thermionic cathodes and of its stability can occur under conditions of industrial interest. It is important to study these patterns in a wide range of conditions and to find out in what conditions each pattern occurs and how a transition between different patterns happens. This work is dedicated to this task. The outline of the paper is as follows. The model for the calculation of steady-state current transfer and its stability and its numerical realization are described in section 2. Numerical results on variations of the pattern of current transfer are given and discussed in section 3. In section 4, a comparison with available experimental data is given and the possibilities of comparison with data of future experiments are discussed. Concluding remarks are given in section 5.

2. Model and numerics

2.1. Equations and boundary conditions

Analysis of this work is based on the model of nonlinear surface heating, which has been virtually universally accepted by now as an adequate tool for analysis of plasma–cathode interaction in high-pressure arc discharges. A detailed description of the model can be found elsewhere (e.g. [9] and references therein; one may find useful also the site [14] where some additional theoretical materials are posted, as well as hints

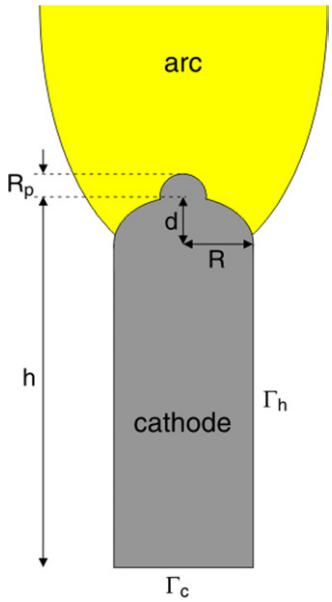

Figure 1. Geometry of the problem.

concerning numerical modelling on the basis of this model). In brief, the model of nonlinear surface heating may be described as follows. Let us consider a thermionic cathode of a high-pressure arc discharge made of a substance of thermal conductivity κ, density ρ and specific heat c_p, which are known functions of the temperature T: $\kappa = \kappa(T)$, $\rho = \rho(T)$, $c_p = c_p(T)$. Joule heat generation inside the cathode is neglected; see, e.g. estimates in [9]. The temperature distribution in the body of the cathode is governed by the non-stationary equation of heat conduction

$$\rho c_p \frac{\partial T}{\partial t} = \nabla \cdot (\kappa \nabla T), \tag{1}$$

where t is time.

The base Γ_c of the cathode is maintained at a fixed temperature T_c by external cooling and the rest of the cathode surface, Γ_h, is in contact with the plasma (or the cold gas) and exchanges energy with it and collects electric current, see figure 1. Then equation (1) is solved with the following boundary conditions:

$$\Gamma_c : T = T_c, \qquad \Gamma_h : \kappa \frac{\partial T}{\partial n} = q(T_w, U). \tag{2}$$

Here n is a direction locally orthogonal to the cathode surface and directed outside the cathode, $q(T_w, U)$ is the density of the energy flux coming from the plasma to the current-collecting part of the cathode surface, T_w is the (local) temperature of the cathode surface and U is the voltage drop across the near-cathode layer (which is assumed to be the same at all points of the arc attachment).

The arc current I is determined by the temperature distribution of the cathode surface and by the value of U and is given by the formula

$$I = \int_{\Gamma_h} j(T_w, U)\, \mathrm{d}S, \tag{3}$$

where $j(T_w, U)$ is the density of electric current to the current-collecting part of the cathode surface.

Densities of the energy flux and of the electric current to the cathode surface, q and j, are treated as known functions of the local surface temperature and of the voltage drop across the near-cathode layer: $q = q(T_w, U)$ and $j = j(T_w, U)$. The arc current I is treated as a given parameter and the problem (1)–(3) is solved for the function T and the parameter U.

Results reported in this work include steady-state solutions to the problem (1)–(3) and their stability against small perturbations. The problem governing steady-state solutions is obtained by dropping the left-hand side of equation (1). The stability was investigated in the framework of the linear theory, which amounts to representing a solution to the problem (1)–(3) as a sum of a steady-state solution T_0 and a small perturbation with an exponential time dependence: $T(\boldsymbol{r}, t) = T_0(\boldsymbol{r}) + T_1(\boldsymbol{r})\mathrm{e}^{\lambda t}$. (Here $\boldsymbol{r}$ denotes the space vector.) The amplitude $T_1(\boldsymbol{r})$ and the increment λ of growth of the perturbation are governed by an eigenvalue problem which is obtained by linearizing the problem (1)–(3) with respect to T_1; see equations (8)–(11) of [22]. (Note that there is a misprint in equation (9) of [22]: the term $T_1(\mathrm{d}\kappa/\mathrm{d}T)(T_0)(\partial T_0/\partial n)$ is missing on the left-hand side.)

2.2. *Numerical solution*

Numerical calculations reported in this work have been performed with the use of the commercial finite element software COMSOL Multiphysics. The functions $q = q(T_w, U)$ and $j = j(T_w, U)$ were calculated by means of equations describing the near-cathode layer in a high-pressure arc plasma that are summarized in [27]. Note that the energy flux related to the vaporization/condensation of the electrode material was neglected in accordance with the estimates [28]. A module realizing this calculation is written in Fortran and the produced data are transferred to COMSOL Multiphysics in the form of tables.

A numerical calculation of steady-state modes of current transfer with investigation of their stability by means of COMSOL Multiphysics was reported in [22, 29]. In [22], the problem (1)–(3) was solved by means of COMSOL Multiphysics through the heat transfer application mode with the use of the stationary and eigenvalue solvers. This approach does not allow one to manually introduce the eigenvalue problem for perturbations; this problem is generated by the software. In [29], the steady-state problem was solved through the heat transfer application mode (or the PDE mode) with the use of the stationary solver, and the eigenvalue problem for perturbations (which was introduced manually) was solved by means of the PDE mode with the use of the eigenvalue solver. Such separation of the steady-state and eigenvalue problems allows one to treat cases where a steady-state mode and its perturbations possess different symmetries, a situation frequently occurring on axially symmetric cathodes.

In particular, such separation allowed an investigation of stability of steady-state 3D modes (which possesses planar symmetry) against antisymmetric perturbations [29], which was lacking in [22]. For completeness, we give here a brief

summary of the results. At the bifurcation point, where the 3D mode being investigated branches off from an axially symmetric mode, all the perturbations are harmonic, i.e. depend on the azimuthal angle φ as $\sin n\varphi$, $n = 1, 2, 3, \ldots$, and there is an infinite number of perturbations with each n. At states beyond the bifurcation point, perturbations are no longer harmonic in φ. They continue to be odd and periodic; however, the period is not necessarily the same as it was at the bifurcation point ($2\pi/n$). The set of periods of odd perturbations of a steady state with ν spots at the edge of the front surface of the cathode is contained between 2π and $2\pi/\nu$ and defined by the same rule as periods of even perturbations; see appendix C of [21]. Odd perturbations do not change sign of their increment along 3D steady-state spot modes. A state with ν spots is neutrally stable against one of the modes of perturbations with the period of $2\pi/\nu$ and stable against the other modes with the same period. If $\nu \geqslant 2$, then this state is unstable against $\nu - 1$ modes of perturbations with periods exceeding $2\pi/\nu$ and stable against all the other modes with such periods. These results, which conform to the analytical theory [21], confirm the reasoning given at the end of section 4.5 of [22] and therefore conclusions on stability drawn in [22] remain unaltered.

In this work, the steady-state problem and the eigenvalue problem for perturbations are solved separately, similarly to how it was done in [29]. The treatment is focused on axially symmetric steady states (note that the states treated in [29] were 3D) and the use is made of the fact that 3D perturbations of axially symmetric steady states are harmonic with respect to the azimuthal angle. The eigenvalue problems governing stability against each of the harmonics may be formulated in 2D; cf equations (20) and (21) of [21]. Therefore, it is sufficient to solve a series of 2D eigenvalue problems governing stability against different harmonics, in order to obtain a complete spectrum of perturbations of an axially symmetric steady state. An obvious advantage of this approach, compared with a straightforward solution of the eigenvalue problem for 3D perturbations in 3D, is a dramatic reduction in RAM and CPU time. Even more important is the elimination of difficulties originating in an extreme sensitivity of results of 3D stability calculations with respect to details of the steady-state solution in the vicinity of the axis of symmetry.

3. Variations of the pattern of current transfer

Numerical results given in this work refer to cathodes made of tungsten. Data on thermal conductivity and emissivity of tungsten have been taken from [30] and [31], respectively. Data used for ρ and c_p affect values of the increment of perturbations, but they do not affect the sign of the increment and, therefore, conclusions on stability. Nevertheless, we indicate for completeness that in this work the density of tungsten was set equal to $19\,250\,\mathrm{kg\,m^{-3}}$ and the specific heat of tungsten was taken from [31]. The value of 4.55 eV was assumed for the work function of tungsten. All the results unless otherwise specified refer to an arc operating in argon under the pressure of 1 bar.

The aim of this section is to investigate variations of the pattern of current transfer to thermionic cathodes. To this end, it is appropriate to consider axially symmetric cathodes which consist of a cylindrical section, a tip in the form of half of a spheroid (ellipsoid of revolution) at the top of the cylindrical section, and a hemispherical protrusion at the top of the tip; see figure 1. (More precisely, the protrusion represents a part of a sphere which is a little bigger than the hemisphere.) The radius and height of the cylindrical section are designated R and, respectively, $h - d$. The axis of revolution of the spheroidal tip coincides with the axis of the cylindrical section, the horizontal semi-axis of the spheroid equals the radius R of the cylindrical section and the vertical semi-axis of the spheroid is designated d. The centre of the hemispherical protrusion is positioned at the height h with respect to the cathode base on the (common) axis of symmetry of the cylindrical section and the tip. The radius of the protrusion is designated R_p. Note that h denotes the height of the cathode without protrusion.

Given a large number of variable control parameters, the following approach was adopted in order to present the results in a manageable way: one variant is chosen as basic (reference point) and then control parameters are varied one by one, each time starting from the basic variant. In order that this approach allow one to demonstrate all kinds of variations of the pattern of current transfer, care should be employed while choosing the basic variant. In this work, the following variant is chosen as basic: $h = 10\,\mathrm{mm}$, $R = d = 1\,\mathrm{mm}$, $R_p = 0$ (that is, a cathode with a hemispherical tip without protrusion), $T_\mathrm{c} = 1000\,\mathrm{K}$.

3.1. Basic variant

Two axially symmetric steady-state modes have been found in numerical simulations for the above-specified basic variant. CVCs and the dependence of the maximum temperature of the cathode surface on the arc current for these two modes are shown in figure 2, U_1 and T_1 referring to one of these modes and U_2 and T_2 to the other. Stable and unstable sections of each mode in this and the following figures are depicted by solid or, respectively, dotted lines. Note that the section of the CVC corresponding to the unstable section of mode 2 coincides, with the graphic accuracy, with the CVC of mode 1 and cannot be seen; the same applies to some of the subsequent figures.

Mode 1 is associated with a smooth distribution of temperature along the front surface of the cathode and is conventionally termed the diffuse mode (although the terms 'pseudodiffuse' or 'fundamental' mode would be more rigorous [32]). It exists and is stable in the whole current range under consideration. Mode 2 is associated with a distribution of temperature with a maximum at the centre of the front surface of the cathode and may be termed the first axially symmetric spot mode. It is composed of two branches separated by a turning point K_1 and exists in a limited current range $I \lesssim 7.6\,\mathrm{A}$. In the following, branches of the spot mode which manifest higher or, respectively, lower values of the maximum temperature of the cathode surface will be referred to as a high- or low-temperature branch.

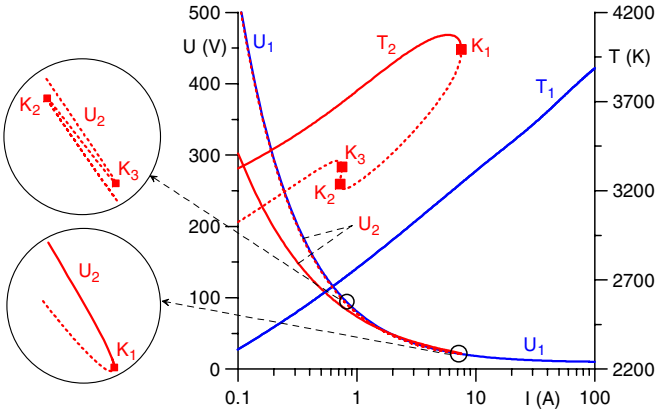

Figure 2. Current–voltage characteristics and maximum temperature of the cathode surface. Cathode with a hemispherical tip, $d = R = 1$ mm, $h = 10$ mm, $T_c = 1000$ K. Squares: turning points.

The high-temperature branch is stable, the low-temperature branch is unstable. The high-temperature branch is associated with a well-pronounced spot, the low-temperature branch is associated with a spot which is somewhat diffuse. The low-temperature branch manifests a shape that resembles Z (the reflected S). The insets in figure 2 show the behaviour of the CVC of the spot mode in the vicinity of the turning point K_1 and in the vicinity of the Z-shape. The near-cathode voltage drop on the high-temperature branch of the spot mode is in the vicinity of the turning point slightly higher than the voltage drop on the low-temperature branch (although this difference is small and can be clearly seen only in the inset), and is lower than the voltage drop on the low-temperature branch at $I \lesssim 1.5$ A.

Except for the Z-shape, this pattern is similar to the one previously established for a rod cathode with a flat front surface [16, 17]. However, there is a fundamental difference concerning stability of the spot mode: both branches of the first axially symmetric spot mode on a cathode with a flat front surface are unstable [22].

Under conditions of figure 2, the high-temperature branch is stable, i.e. all perturbation modes have negative increments. It follows from the theoretical analysis of stability in the vicinity of a turning point [21, 32] that there are one axially symmetric perturbation mode with a positive increment on the section K_1K_2 of the low-temperature branch; two axially symmetric perturbation modes with positive increments on the section K_2K_3 and one axially symmetric perturbation mode with a positive increment beyond the turning point K_3. This is indeed what has been found in the numerical modelling. No 3D perturbation modes with positive increments have been found.

Under conditions of figure 2, states in the vicinity of the turning point K_1 that are associated with higher values of the near-cathode voltage and maximum temperature of the cathode surface are stable, and those associated with lower values are unstable. However, the theoretical analysis [21] indicates that stability of a state in the vicinity of a turning point is unrelated to whether this state is associated with lower or higher values of the near-cathode voltage or maximum temperature of the cathode surface: what matters is whether the turning point in the plane (I, U) is traversed in the clockwise direction or in the counterclockwise direction. In the former case, states before the turning point are stable against one mode of perturbations of the same symmetry that the steady-state mode itself and states after the turning point are unstable. In the latter case, states before the turning point are unstable and the ones after it are stable. Therefore, the above-mentioned feature of figure 2 is not a general result. Indeed, counter-examples will be encountered in the following.

The above-described modelling predicts stable regimes of current transfer at currents of several hundred milliamperes with near-cathode voltages of several hundred volts, far in excess of near-cathode voltages of up to 50 to 60 V observed in experiments with arc cathodes (e.g. [18, 33]). One should keep in mind, however, that although the current range of several hundred milliamperes has been studied experimentally in connection with high-intensity discharge lamps (e.g. [34]), this was done on substantially smaller cathodes (of a radius of a few hundred micrometres), i.e. at substantially higher average current densities. On the other hand, this current range is well above the range of a few milliamperes, which is characteristic of dc atmospheric-pressure glow discharges (e.g. [35–37]). Thus, the above regimes are intermediate between those characteristic for arc and glow cathodes and remain unexplored, to the best of our knowledge. It would be very interesting to try to observe such regimes experimentally. (Note that effects neglected by the present model come into play in such regimes, e.g. secondary electron emission and deviations of the electron energy distribution function from the Maxwellian distribution. These effects, however, can hardly render theoretical predictions inaccurate by orders of magnitude. Note that it is not very difficult to include these effects in the model if needed.)

This is one of the reasons why the CVCs are shown in figure 2 and subsequent figures in the range of near-cathode voltages of up to 500 V, a value unusually high from the point of view of arc cathodes. Another reason is that the nature of variations of patterns of current transfer cannot be understood without the analysis of data referring to a wide range of conditions, as will be seen in the following.

In addition to the two above-discussed axially symmetric solutions describing the diffuse mode and the first axially symmetric spot mode, also 3D solutions describing 3D spot modes have been found in the modelling. However, the position of the maximum of the temperature of the cathode surface, described by these solutions, in most cases was found to coincide with the position of the maximum in the initial approximation used to compute the corresponding solution. In other words, it was possible to obtain a solution with a spot positioned at virtually any point of the front surface of the cathode. The set of multiple solutions was discrete in all the cases studied before; therefore, the existence of a continuum set of 3D spot modes is unexpected and this result requires a special analysis. Such analysis falls beyond the scope of this work; therefore, the following treatment is focused on axially symmetric modes.

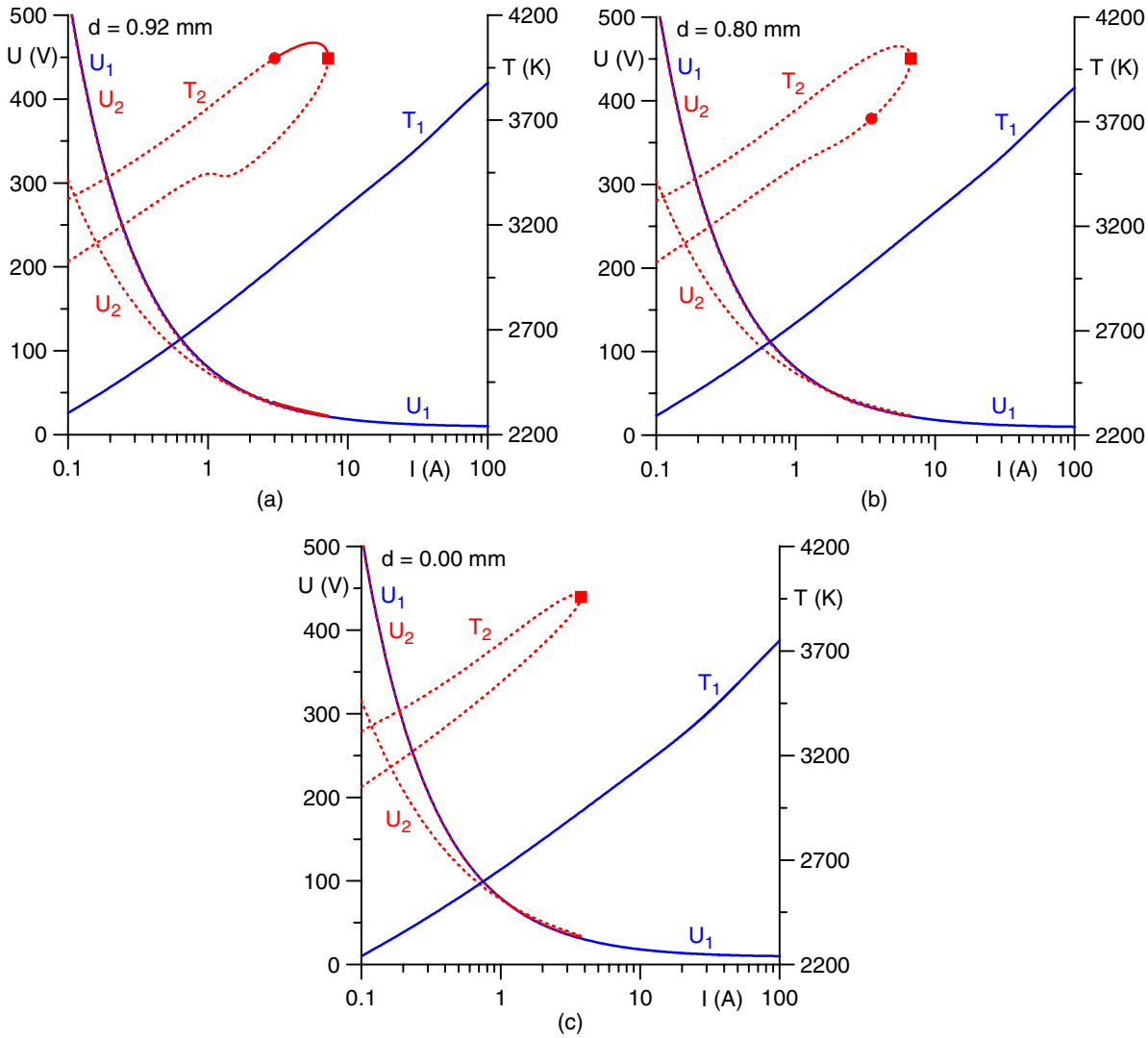

Figure 3. Effect of curvature of the cathode tip on the pattern of steady-state modes of current transfer to cathodes with oblate spheroidal tips (*a*), (*b*) and a flat tip (*c*). Circle: state at which the change in stability against the first mode of 3D perturbations occurs. Square: turning point. $R = 1$ mm, $h = 10$ mm, $T_c = 1000$ K.

3.2. Effect of the curvature of the cathode tip

The curvature of the cathode tip is defined by the parameter d (see figure 1): $d = R$ corresponds to a hemispherical tip, $0 < d < R$ to an oblate spheroidal tip, $d = 0$ to a cathode with a flat front surface and $d > R$ to a prolate spheroidal tip.

3.2.1. Oblate spheroidal tip. CVCs and the dependence of the maximum temperature of the cathode surface on the arc current for several cathodes with $d < R$ are shown in figure 3. In all the cases, the indices 1 and 2 continue to designate the diffuse and, respectively, the first axially symmetric spot modes.

A decrease in the curvature of the cathode tip has virtually no effect on the diffuse mode and its stability. There is some effect over the spot mode: the above-described Z-shape which is present on the low-temperature branch of the spot mode in the basic variant (at $d = 1$ mm) becomes less pronounced with a decrease in d and has been extinguished already at $d = 0.98$ mm. The weak non-monotony of the dependence $T(I)$ on the low-temperature branch of the spot mode which is seen in figure 3(*a*) at I between approximately 1 and 2 A represents a 'remnant' of the Z-shape. Otherwise, the effect of a decrease in the curvature of the cathode tip over the spot mode is not strong. Similarly to what is seen in figure 2, the near-cathode voltage drop on the high-temperature branch of the spot mode is in all the cases slightly higher than the voltage drop on the low-temperature branch in the vicinity of the turning point (although this difference is small and can hardly be seen in figures 3(*a*)–(*c*)), and is lower than the voltage drop on the low-temperature branch at I below approximately 1.5 A.

There is, however, a dramatic effect over stability of the spot mode. In the basic variant, the high-temperature branch is stable against all perturbations and the low-temperature branch is unstable against axially symmetric perturbations, with the change in stability occurring at the turning point separating these branches. As d decreases, states of the high-temperature branch lose stability against the perturbations proportional to sine or cosine of the azimuthal angle, which represent the first

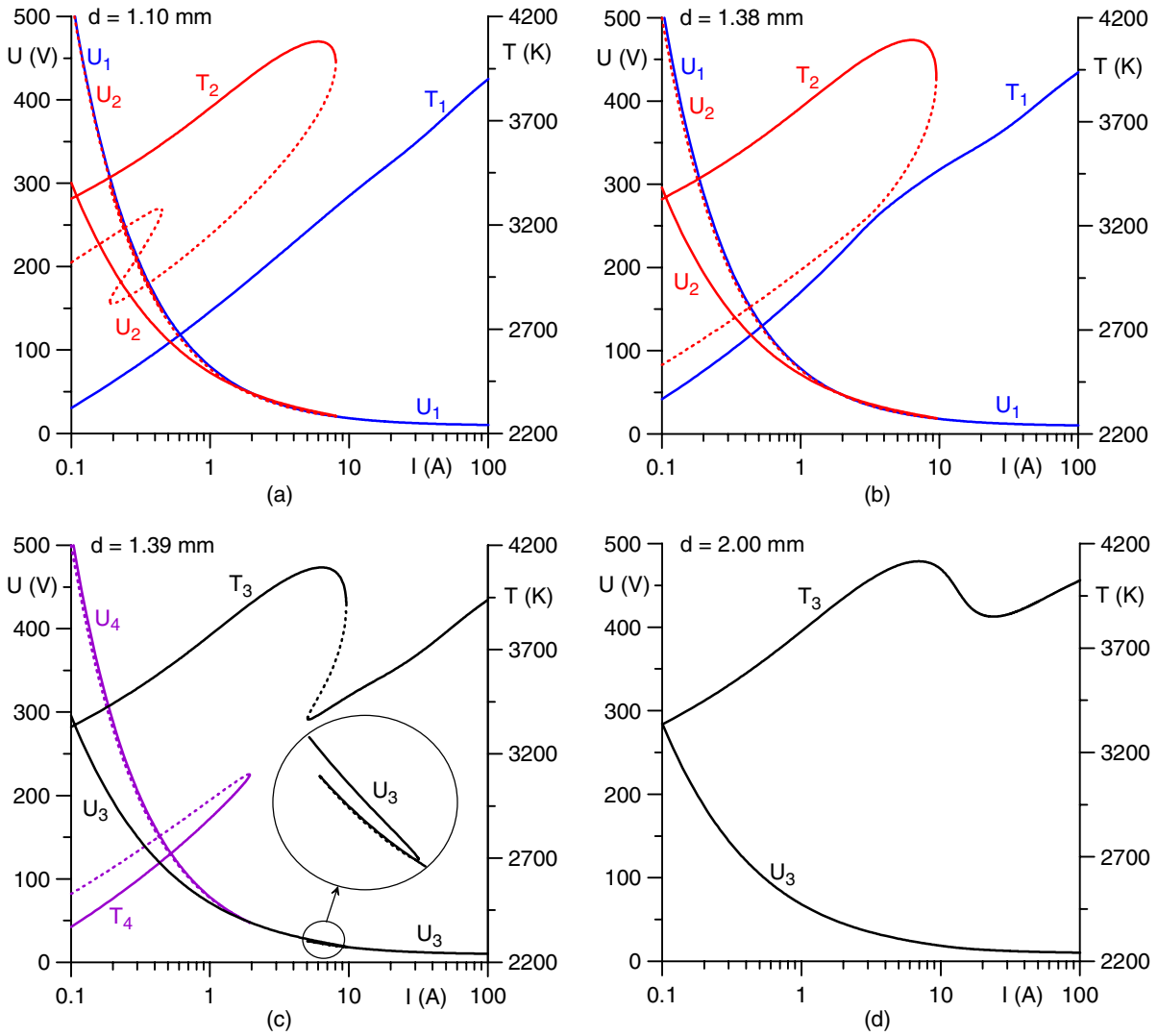

Figure 4. Effect of curvature of the cathode tip on the pattern of steady-state modes of current transfer to cathodes with prolate spheroidal tips. $R = 1$ mm, $h = 10$ mm, $T_c = 1000$ K.

mode of 3D perturbations. The state at which the change in stability against the first mode of 3D perturbations occurs is marked in figure 3 by a circle. (Note that a bifurcation of steady-state modes of current transfer occurs at this state: a 3D steady-state mode branches off from the first axially symmetric spot mode.) Initially, this state is positioned in the region of low currents; see figure 3(*a*): the high-temperature branch is unstable at lower currents but still stable between the point of change of stability against the first mode of 3D perturbations and the turning point. As d decreases further, the point of change of stability moves in the direction of the turning point; the stable section of the high-temperature branch shrinks. At $d \approx 0.88$ mm the point of change of stability passes over the turning point and moves to the low-temperature branch; the whole of the high-temperature branch becomes unstable.

At still smaller d, the point of change of stability against the first mode of 3D perturbations is shifted in the direction of low currents and eventually displaced from the graph; figure 3(*c*). This is a situation familiar from simulations for the cathode with a flat front surface [22]: the high-temperature branch of the first axially symmetric spot mode is unstable against the first mode of 3D perturbations; the low-temperature branch is unstable against the first mode of 3D perturbations and axially symmetric perturbations (and, at low currents, also against higher modes of 3D perturbations).

The above results reveal the first possible scenario of variation of the pattern of current transfer to thermionic cathodes: a change in stability of the first axially symmetric spot mode which occurs through a travel of the point of change of stability against the first mode of 3D perturbations along the whole spot mode.

3.2.2. Prolate spheroidal tip. CVCs and the dependence of the maximum temperature of the cathode surface on the arc current for prolate tips, $d > R$, are shown in figure 4. As d increases from 1 mm upwards (figure 4(*a*)), the above-described Z-shape which is present on the low-temperature branch of the spot mode in the basic variant (figure 2) becomes better pronounced and simultaneously is shifted in the direction of low currents. As d increases further, the Z-shape is shifted into the range $I < 0.1$ A and disappears from the graph (figure 4(*b*)).

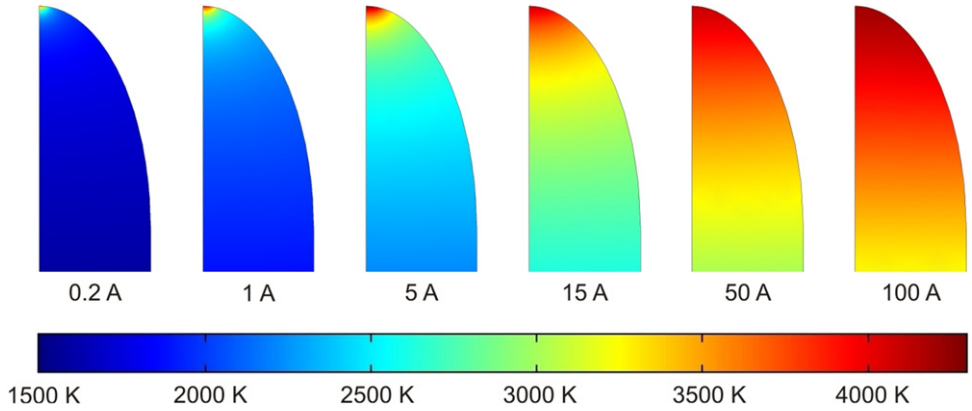

Figure 5. Distributions of the temperature inside a cathode with a prolate spheroidal tip in states belonging to mode 3. $d = 2$ mm, $R = 1$ mm, $h = 10$ mm, $T_c = 1000$ K.

Another effect caused by an increase in d and seen in figures 4(a) and (b) is approaching of the diffuse and spot modes. At $d \approx 1.383$ mm the two modes become connected: there is a state, corresponding to $I \approx 3.63$ A, which belongs to both modes. In other words, a bifurcation occurs. There are two disconnected modes once again as d grows further (figure 4(c)); however, we will see that these modes cannot be identified with the diffuse and spot modes. The mode to which the index 3 refers exists in the whole current range under consideration and possesses a Z-shape. It is stable with the exception of the 'retrograde' section of the Z-shape (the section between the turning points). The mode to which the index 4 refers exists only at low currents and comprises two branches separated by a turning point. Again, the branch which manifests higher or, respectively, lower values of the maximum temperature of the cathode surface will be referred to as the high- or low-temperature branch. The low-temperature branch is stable in this case (and is represented by the solid line) while the high-temperature branch is unstable (and is represented by the dotted line), in contrast to what happens in the case of the spot mode depicted in figures 2, 4(a), and 4(b). The high-temperature branch of mode 4 in the whole range of existence of this mode is associated with a slightly lower near-cathode voltage drop than the low-temperature branch, although the difference is small and can hardly be seen in figure 4(c).

As d increases, the Z-shape on mode 3 becomes less pronounced and is eventually extinguished (figure 4(d)). Mode 4 is shifted in the direction of low currents; eventually it is displaced from the graph and only one mode exists in the whole current range considered (figure 4(d)). Since this mode possesses no Z-shapes, only one thermal regime of the cathode is possible at any current value within the range considered. It is interesting that this mode manifests a minimum in the dependence of the temperature of the hottest point of the cathode on the arc current, positioned at $I \approx 23.9$ A.

Apart from the Z-shapes that may be present on mode 2 (spot mode) and mode 3, the CVCs of modes 3 and 4 shown in figures 4(c) and (d) are not fundamentally different from the CVCs of the diffuse and, respectively, spot modes in figures 2, 4(a) and 4(b). However, the maximum cathode temperature in mode 3 at all currents exceeds the maximum temperature on

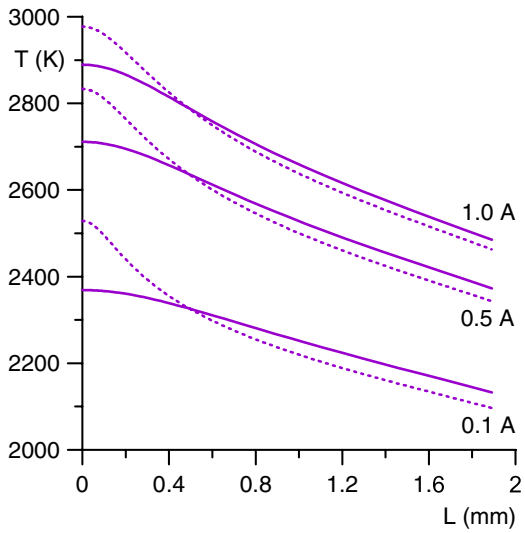

Figure 6. Distributions of the temperature along the surface of a cathode with a prolate spheroidal tip in states belonging to mode 4. Solid: stable (low-temperature) branch. Dotted: unstable (high-temperature) branch. $d = 1.39$ mm, $R = 1$ mm, $h = 10$ mm, $T_c = 1000$ K.

both branches of mode 4, and this does not allow one to identify mode 3 with the diffuse mode and mode 4 with the first axially symmetric spot mode. Temperature distributions in the body of the cathode for several states belonging to mode 3 are shown in figure 5. While high-current states are characterized by smooth temperature distributions typical for the diffuse mode, there is a well-defined spot in the low-current states. A comparison of the distributions of the temperature of the cathode surface for states with the same current belonging to the stable, or low-temperature, and unstable, or high-temperature, branches of mode 4 is shown in figure 6. (Here L is the distance to the centre of the front surface of the cathode measured along the generatrix.) States belonging to the stable branch are characterized by smooth temperature distributions typical for the diffuse mode and there is something resembling a poorly pronounced spot on the unstable branch.

In other words, each of the two modes of steady-state current transfer existing in this geometry embraces diffuse

states and states with spots; a result similar to the one reported in [23] for a cathode with a protrusion on the top of a hemispherical tip.

One should emphasize that the above-described bifurcation occurring at $I \approx 3.63$ A in the case $d \approx 1.383$ mm involves modes of the same symmetry and occurs at only one value of the parameter d. In this respect, this bifurcation is fundamentally different from the pitchfork (symmetry-breaking) and saddle-node bifurcations already encountered in the theory of axially symmetric arc cathodes [15, 21]. One can see from figures 4(*b*) and (*c*) that the modes exchange branches at this point, and this is why each of the two modes at $d > 1.383$ mm embraces states typical for both diffuse and spot modes.

The above results reveal the second possible scenario of variation of the pattern of current transfer to thermionic cathodes: a bifurcation that is not symmetry-breaking occurs at a particular value of a control parameter (d, in this case) and is accompanied by an exchange of branches.

3.3. Effect of the cathode radius and height

Simulations reported in this section have been performed for a cathode with a hemispherical tip, $d = R$, at $T_c = 1000$ K. First, the cathode radius R was varied at a fixed height $h = 10$ mm. Second, the height h was varied at a fixed radius $R = 1$ mm. The results of the simulations were the following. (The corresponding graphs are not given here in order not to overload the paper.)

The effects of increase in the radius from 1 mm upwards and of decrease in the height from 10 mm downwards are both quite similar to the effect of increase in the curvature of the cathode tip at a fixed R and h. The Z-shape which is present on the low-temperature branch of the spot mode in the basic variant (figure 2) becomes better pronounced and simultaneously shifted in the direction of low currents. The diffuse and spot modes approach each other and a bifurcation that is not symmetry-breaking appears (at an R value somewhere between 1.16 mm and 1.17 mm or, respectively, at an h value between 8.32 mm and 8.33 mm). This bifurcation is accompanied by an exchange of branches, so each of the two modes emerging at $R \gtrsim 1.17$ mm or, respectively, $h \lesssim 8.32$ mm embraces states typical for both diffuse and spot modes. In other words, the second above-described scenario occurs.

A decrease in the cathode radius from 1 mm downwards and an increase in the height from 10 mm upwards do not cause dramatic changes in the pattern of modes of current transfer. The diffuse and spot modes continue to exist separately. The Z-shape which is present on the low-temperature branch of the spot mode in the basic variant (figure 2) becomes less pronounced and eventually is extinguished. The turning point of the spot mode is shifted in the direction of low currents. There is no effect on the stability: the diffuse mode is stable, the high-temperature branch of the spot mode is stable and the low-temperature branch is unstable. Note that some of these features are similar to those characteristic of the decrease in the curvature of the cathode tip at fixed R and h (the separate existence of the diffuse and spot modes and the disappearance of the Z-shape), while the others are different (the shift of the turning point of the spot mode and the lack of effect over stability).

3.4. Effect of a protrusion at the top of the cathode tip

In this section, a cathode in the form of a rod with a hemispherical tip and a hemispherical protrusion is considered and modelling results are given for different radii of the protrusion, all the other parameters being fixed. CVCs and the dependence of the maximum temperature of the cathode surface on the arc current are shown in figure 7. Temperature distributions in the body of the cathode for several states belonging to mode 3 under conditions of figure 7(*e*) are shown in figure 8.

Let us first compare figure 7(*a*) with figure 2. The presence of a protrusion produces virtually no effect over the diffuse mode and a strong effect over the spot mode. First, the maximum temperature attained by the cathode surface on the stable branch of the spot mode is much higher than that under conditions of the basic variant: the temperature of the protrusion exceeds 5000 K under conditions of figure 7(*a*). Second, the spot mode under conditions of figure 7(*a*) possesses three turning points, similarly to the spot mode under conditions of figure 2, and changes its stability at each of these turning points, in contrast to what happens under conditions of figure 2. It is interesting to note that the number of turning points of the spot mode may vary with an increase in the radius of the protrusion; e.g. five turning points are seen in figure 7(*b*).

One can see from figures 7(*a*)–(*e*) that the effect of an increase in the radius R_p of the protrusion is similar to the effect of an increase in the curvature of the cathode tip at fixed R and h or an increase in the ratio R/h of the cathode with a hemispherical tip. The diffuse and spot modes approach each other and a bifurcation that is not symmetry-breaking occurs at an R_p value somewhere between 80 and 85 μm. This bifurcation is accompanied by an exchange of branches, so each of the two modes emerging at $R_p \gtrsim 85\,\mu$m embraces states typical for both diffuse and spot modes. In other words, the second above-described scenario occurs.

3.5. Effect of the temperature of the cathode base

In this section, a cathode of the same geometry that in the basic variant is considered and modelling results are given for different temperatures T_c of the cathode base. CVCs and the dependence of the maximum temperature of the cathode surface on the arc current are shown in figure 9.

Comparing figure 9(*a*) with figure 2, one can see that the decrease in the temperature of the cathode base from 1000 to 750 K has virtually no effect on the diffuse mode. The Z-shape which is present on the low-temperature branch of the spot mode in the basic variant is not seen in figure 9(*a*): it has been shifted to the range of lower currents.

As T_c decreases further, a junction appears between the diffuse and spot modes and these modes form a single mode with a Z-shape; see figure 9(*b*). This mode resembles mode 3

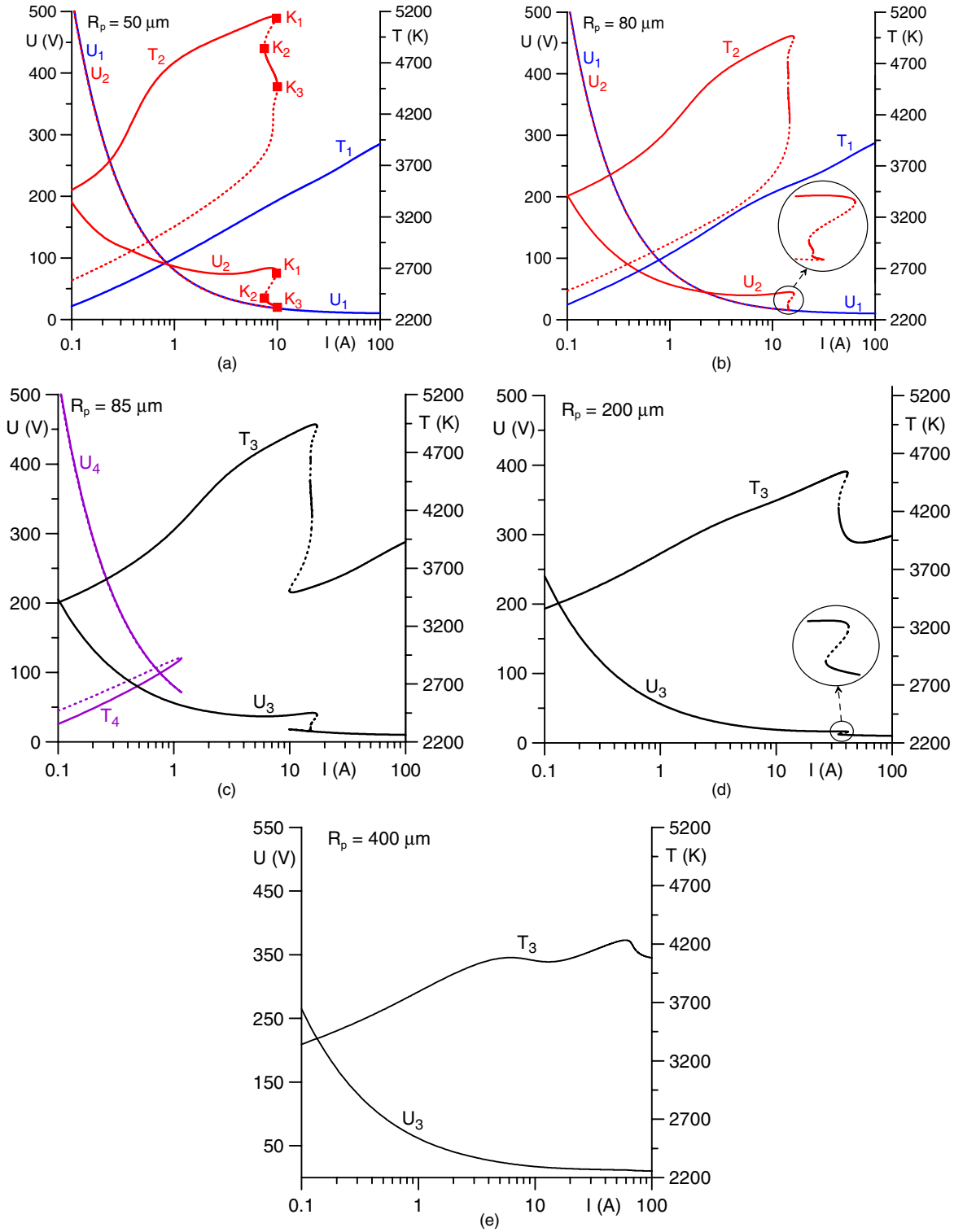

Figure 7. Effect of a protrusion on the top of a hemispherical cathode on the pattern of steady-state modes of current transfer. $d = R = 1$ mm, $h = 10$ mm, $T_c = 1000$ K.

in figures 4(*c*) and 7(*c*) and is attributed the same designation. As T_c decreases still further, the Z-shape on this mode becomes less pronounced and is eventually extinguished (figure 9(*c*)). Skipping for brevity temperature distributions in the body of the cathode for different arc currents under conditions of figure 9(*c*), we only note that mode 3 in these conditions embraces states typical for both diffuse and spot modes, similarly to mode 3 under conditions of figures 4(*c*) and 7(*c*).

In order to investigate the appearance of the junction, modelling was performed for T_c from 750 to 730 K in the current range down to 10 mA. The pattern of solutions at $T_c = 749$ K is similar to the one shown in figure 9(*a*) and

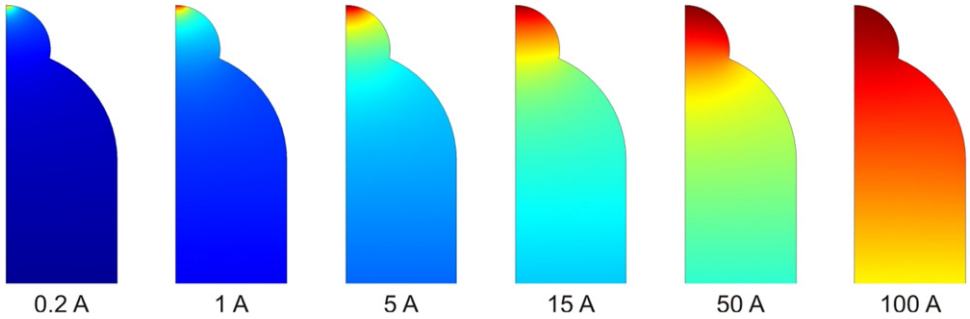

Figure 8. Distributions of the temperature inside a cathode with a protrusion in states belonging to mode 3. $R_p = 400\,\mu$m, $R = 1$ mm, $h = 10$ mm, $T_c = 1000$ K. The temperature bar is shown in figure 5.

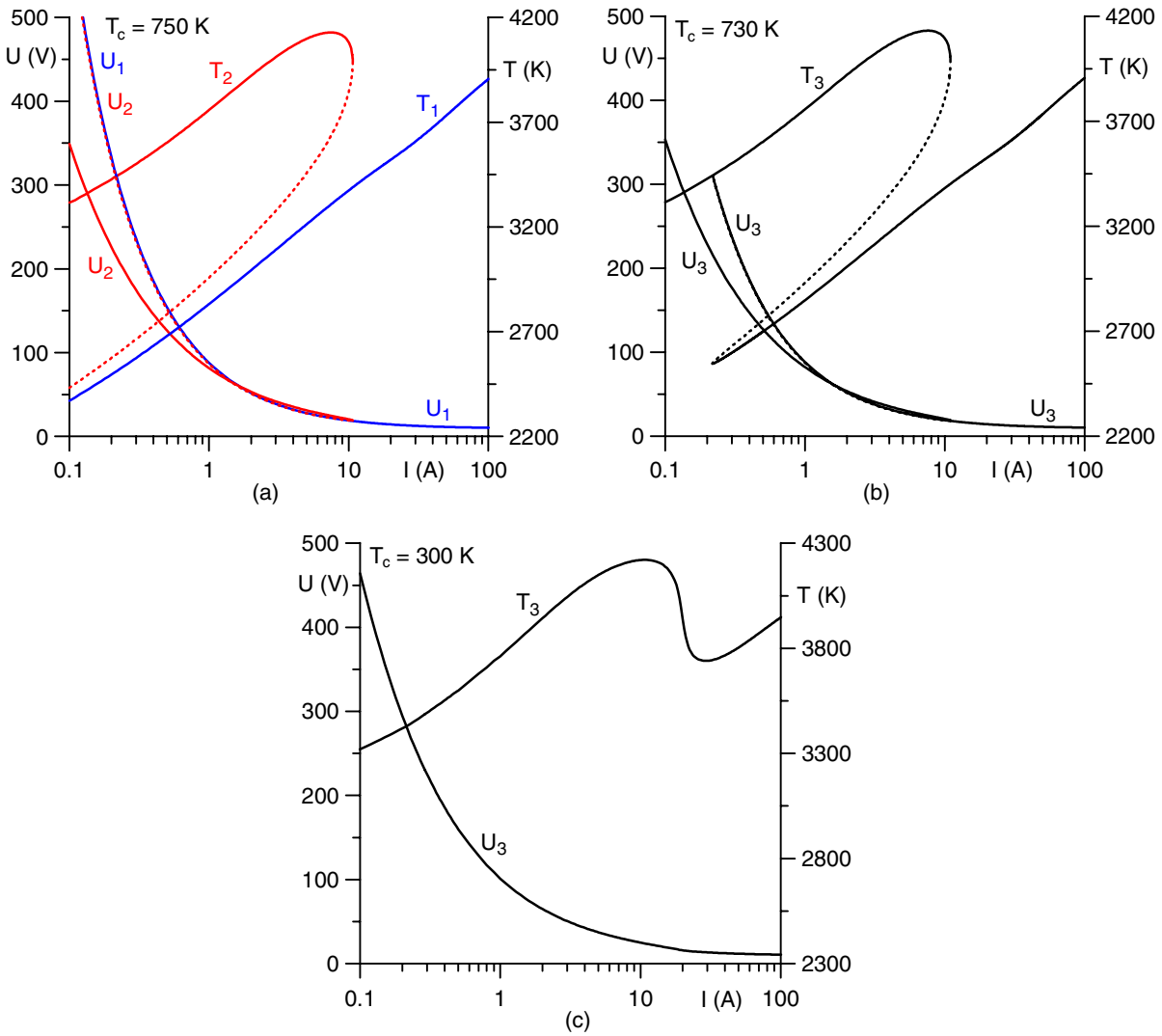

Figure 9. Effect of the temperature of the cathode base on the pattern of steady-state modes of current transfer. Cathode with a hemispherical tip, $d = R = 1$ mm, $h = 10$ mm.

comprises two disconnected modes. At $T_c \leqslant 748$ K, the pattern of solutions is similar to the one shown in figure 9(*b*): there is a single mode with a Z-shape. Note that the junction at $T_c = 748$ K occurs at $I \approx 12$ mA. In other words, the junction of the diffuse and spot modes enters the range of I being considered from the region of very low currents.

Thus, one can identify the third scenario of variation of the pattern of current transfer: a junction of the diffuse and spot modes, the result being a single mode existing in a wide current range and comprising states characteristic of the spot mode at low current and of the diffuse mode at high currents. This mode is similar to mode 3 in the second scenario; however,

there is a difference in the two scenarios as far as the way of its appearance is concerned: through a junction of the diffuse and spot modes that enters the considered range of I from the region of very low currents in the third scenario or through a bifurcation that is not symmetry-breaking and occurs at a certain value of I inside the current range being considered in the second scenario. No analogue of mode 4 exists in the third scenario.

3.6. Discussion

Simulation results reported in this work show that variations of control parameters may dramatically change the pattern of steady-state modes of current transfer to a thermionic arc cathode. Three scenarios of these changes have been found. The first one is the movement of the point of change of stability against the first mode of 3D perturbations along the axially symmetric spot mode. This scenario occurs when the curvature of the front surface of the cathode increases starting from zero at fixed radius and height of the cathode. This movement results in the high-temperature branch of the axially symmetric spot mode, while being unstable on the cathode with a flat front surface, becoming stable on a cathode with a hemispherical front surface.

The second scenario is realized through a bifurcation of the diffuse and axially symmetric spot modes that occurs at a certain combination of control parameters and is not symmetry-breaking. The bifurcation is accompanied by an exchange of branches of the modes, which is why each of the two modes appearing as a result of the bifurcation embraces states typical for both diffuse and spot modes. One of these two modes (mode 3) exists at all currents, possesses a Z-shape, and is stable with the exception of the retrograde section of the Z-shape. The other mode (mode 4) exists only at low currents and comprises two branches separated by a turning point, one of these branches being stable and the other unstable. Further on from the bifurcation point, the Z-shape on mode 3 becomes less pronounced and is eventually extinguished, mode 4 is shifted in the direction of low currents and is eventually displaced into the range $I < 0.1$ A. Thus, only one mode remains in the current range of interest and this mode embraces states with a diffuse temperature distribution at high currents and states with a hot spot at low currents. Since this mode possesses no Z-shapes, only one thermal regime of the cathode is possible at any current value within the range considered and this regime is stable. This scenario was encountered when the curvature of the front surface was increased at a fixed cathode radius and height, when the radius of a cathode with a hemispherical tip was increased at a fixed height, when the height of a cathode with a hemispherical tip was decreased at a fixed radius and when the radius of a hemispherical protrusion on top of a cathode in the form of a rod with a hemispherical tip was increased.

The third scenario is realized through a junction of the diffuse and axially symmetric spot modes, which enters the considered range of arc currents from the region of very low currents. This scenario is similar to the second one except that mode 4 does not appear. This scenario was encountered when the temperature of the cathode base was decreased at fixed geometrical parameters.

The first above-described scenario is intuitively clear: rounding of the cathode tip produces a stabilizing effect over a spot positioned at the centre of the tip. The physical meaning of the second scenario may be understood as follows. There are two reasons for the appearance of concentrations of current in certain parts of the cathode surface, i.e. of current spots: non-uniformities of geometrical and/or physical properties of the current-collecting surface (such as the presence of protrusions or areas with a reduced work function) and self-organization. A cathode with a flat front surface and thermally and electrically insulated lateral surface [15] represents a limiting case in which the current-collecting surface of the cathode is uniform and the first reason is absent. The diffuse mode of current transfer to such a cathode is described by a 1D solution: the temperature in the body of the cathode varies in the axial direction but not in the transversal directions. This solution exists at all arc currents. At arc currents low enough, also axially symmetric and 3D solutions exist describing different spot modes. In other words, a state with uniform distributions of temperature and current density along the front surface exists at any arc current, and at arc currents low enough also states with non-uniform distributions, i.e. self-organization, exist.

In all the cases other than the above-described limiting case, including the case of a cathode with a flat tip and an active lateral surface, the current-collecting surface is geometrically non-uniform. Accordingly, the diffuse mode is multidimensional rather than 1D and is associated with temperature and current density that vary along the cathode surface rather than being constant. One can expect that the non-uniformity, if it is strong enough, is incompatible with the existence of multiple solutions, i.e. with self-organization. Therefore, the second scenario may be understood as a transition from a pattern with two distinct modes, which is a manifestation of self-organization, to a pattern with one mode, which is governed by a non-uniformity of the current-collecting surface. The bifurcation through which this transition is realized may be understood in similar terms: when the non-uniformity of the current-collecting surface reaches a certain level, the cathode temperature distribution associated with the diffuse mode becomes at a certain value of the arc current exactly identical to the temperature distribution associated with the spot mode; the diffuse and spot modes become connected, i.e. a bifurcation occurs. One needs to resort to the general theory of bifurcations in order to understand why this bifurcation is accompanied by an exchange of branches between the diffuse and spot modes; this question is beyond the scope of this work and will be treated elsewhere [32].

The physical meaning of the third scenario is the same: it may be viewed as a transition from a self-organized pattern with two distinct modes, the diffuse mode and the spot mode, to a pattern with a single mode, mode 3, which is governed by a non-uniformity of the current-collecting surface and embraces states with a diffuse temperature distribution at high currents and states with a hot spot at low currents.

An increase in d (at all the other parameters, including the arc current, being fixed) or R_p clearly results in a less

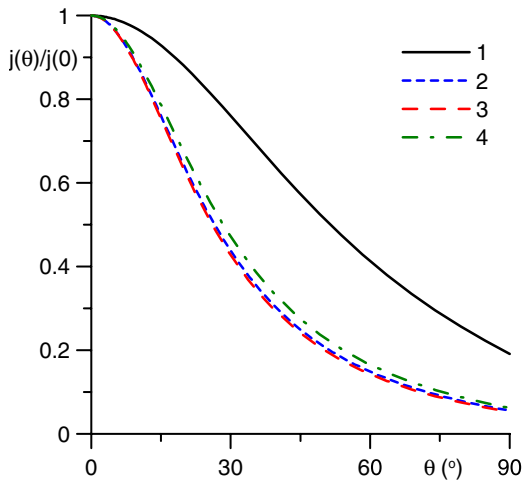

Figure 10. Normalized distributions of the current density over the hemispherical cathode tip. $I = 5$ A. 1: $d = R = 1$ mm, $h = 10$ mm, $T_c = 1000$ K. 2: $d = R = 1.16$ mm, $h = 10$ mm, $T_c = 1000$ K. 3: $d = R = 1$ mm, $h = 8.4$ mm, $T_c = 1000$ K. 4: $d = R = 1$ mm, $h = 10$ mm, $T_c = 700$ K.

uniform current distribution in the diffuse mode. The same effect is produced by an increase in R: the area of the arc attachment is governed primarily by the arc current and does not change much if the current is fixed, while the area of the current-free surface increases. The same effect is produced also by a decrease in h or T_c: a more intense cooling of the arc attachment results in its shrinking. The latter statements are illustrated by figure 10, where distributions of the current density over the hemispherical cathode tip are shown for states corresponding to the same arc current $I = 5$ A. Here θ is the polar angle, $\theta = 0$ and $\theta = 90^\circ$ corresponding to the centre of the tip and, respectively, junction of the tip with the cylindrical lateral surface. Lines 1, 2 and 3 correspond to states belonging to the diffuse mode in, respectively, the basic variant, a variant with an increased R and a variant with a reduced h. Line 4 corresponds to a state belonging to the 'base' of the Z-shape in a variant with a reduced T_c; note that the Z-shape in this variant is localized in the current range $2.3\,\text{A} \lesssim I \lesssim 11.4\,\text{A}$. One can see that the distributions described by lines 2–4 manifest considerably more narrow maxima at the centre of the tip than the distribution described by line 1, i.e. are less uniform.

Thus, in all the cases the evolution of a self-organized pattern with two distinct modes in the direction of a pattern with one mode is accompanied by an increase in non-uniformity of the diffuse mode, in accordance with the above reasoning.

The above reasoning explains the direction of evolution of the patterns caused by a variation of each parameter but does not predict whether this evolution occurs through the second or third scenario. In fact, similar variations of the same parameter may provoke both scenarios, depending on the other parameters. For example, a decrease in h at $d = R = 1$ mm provokes the second scenario when realized at $T_c = 1000$ K (see section 3.3) and the third scenario when realized at $T_c = 300$ K.

According to the above reasoning, the physics of the spot-like arc attachment at low currents in mode 3 and in the spot mode is not quite the same. The spot in the spot mode is a result of self-organization. The corresponding thermal regime is not the only one possible under the conditions considered: a thermal regime with a diffuse temperature distribution is possible as well, and also a thermal regime associated with the other branch of the spot mode. The spot at low currents in mode 3 represents an attachment of the arc to the centre of the cathode tip. No other stationary thermal regime of cathode exists after the Z-shape has disappeared. In fact, mode 3 may be viewed as a diffuse mode with a strongly variable size of the arc attachment. At high currents, which are sufficient to heat up the whole of the cathode tip, the attachment covers the whole front surface of the cathode. At low currents, which suffice to heat up only a small fraction of the cathode tip, the attachment occupies a small fraction of the front surface. This variation of the size of the arc attachment is clearly seen in figures 5 and 8.

4. Comparison with experiment

4.1. Low-current arcs

Results of the present modelling seem to be related to results of experiments [6, 24, 25], which have been performed in low-current arcs typical for high-intensity discharge lamps. The experiments [24, 25] indicate that a protrusion on the front surface of the cathode facilitates a stable operation of the cathode in the spot mode, in particular, helps to eliminate flickering. In [6], three modes of current transfer were observed: the diffuse mode, the spot mode and a new mode called by the authors the super spot mode. The cathodes were manufactured as rods with a flat tip. After operation in the spot mode, the edge of the front surface became rounded due to local melting. After some hours of operation in the spot mode, structures of the dimension of about 20–200 μm appeared, which were interpreted as attachment locations for the super spot mode. Data of thermal measurements in the spot and super spot modes taken from figure 15 of [6] are shown in figures 11(*a*) and (*b*). The super spot mode manifests significantly decreased global cathode tip temperature and significantly decreased total power losses of the cathode (power removed from the cathode by heat conduction and radiation). The latter means that this is the most efficient mode of cathodic arc attachment.

Also shown in figure 11 are modelling results. In accordance with the experimental observations, the following four variants of the cathode geometries were considered: a rod with a flat front surface; a rod with a front surface which is flat at the centre and rounded at the edge, the radius of rounding being 100 μm; a cathode with a hemispherical tip and a hemispherical protrusion of a 100 μm radius located on top of the tip; a cathode with a hemispherical tip and a protrusion in the form of half of a prolate spheroid with minor and major semi-axes of 50 μm and 150 μm, respectively. It was set $R = 0.75$ mm, $h = 19$ mm, $T_c = 300$ K in all the variants.

In the first and second variants two separate modes were found, the diffuse mode and a 3D spot mode with a spot at the edge of the front surface of the cathode localized in the

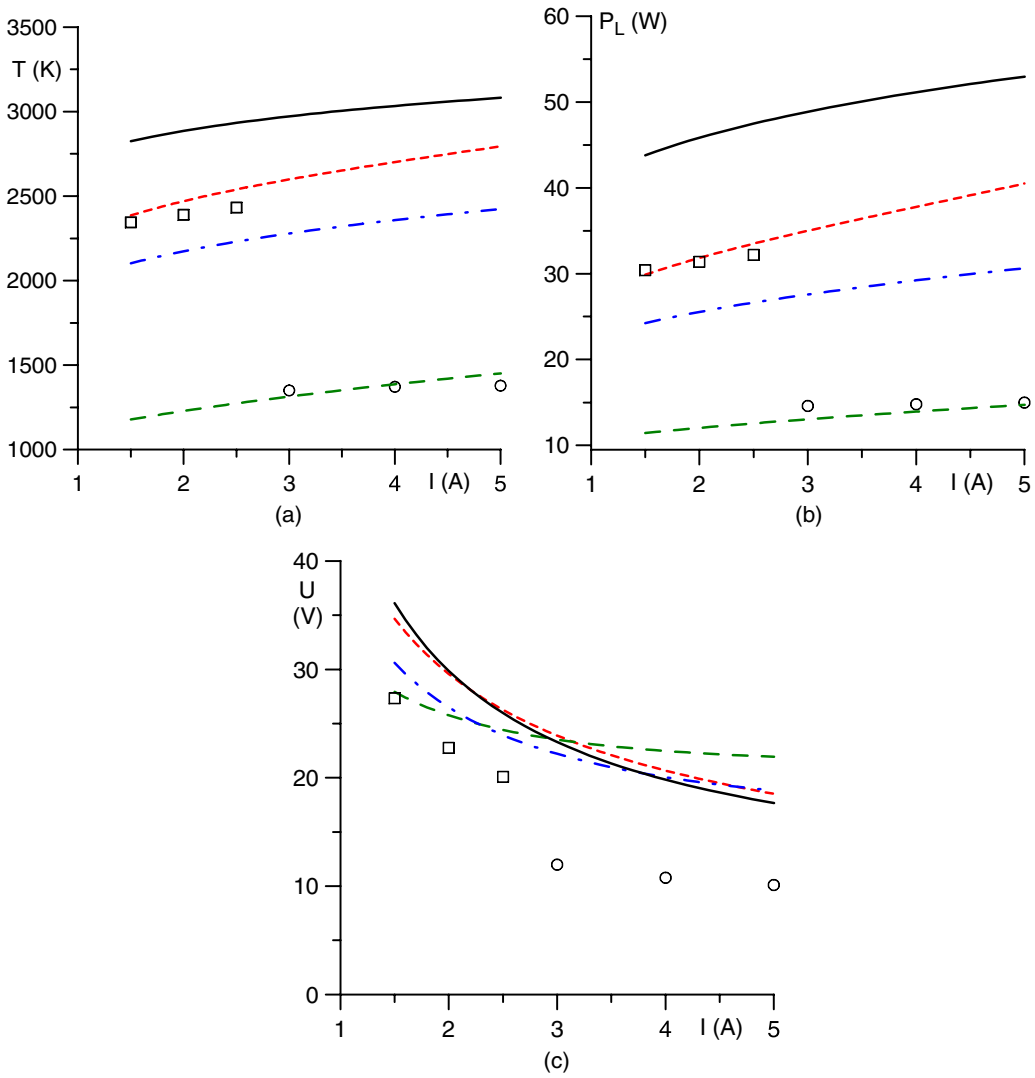

Figure 11. Characteristics of tungsten cathodes operating in a xenon plasma under the pressure of 2.6 bar. $R = 0.75$ mm, $h = 19$ mm, $T_c = 300$ K. Lines: modelling. Points: experiment [6]. Solid: diffuse mode. Short-dashed, dot-dashed, and squares: spot mode. Circles: super spot mode. Long-dashed: mode 3. (*a*) Global cathode tip temperature. (*b*) Total power losses. (*c*) CVC.

current ranges $I \lesssim 10.4$ A and, respectively, $I \lesssim 6.8$ A. Two separate modes were also found in the third variant, the diffuse mode and an axially symmetric spot mode with a spot at the centre localized in the current range $I \lesssim 12.5$ A. In the fourth variant, mode 3 was found with two Z-shapes localized in the current range 15.6 A $\lesssim I \lesssim$ 39.2 A. The solid lines in figure 11 represent modelling data on the diffuse mode under conditions of the first variant (which coincide, to the graphic accuracy, with similar data under conditions of the second variant). The short-dashed lines represent the high-temperature branch of the 3D spot mode under conditions of the second variant. The dot–dashed lines represent the high-temperature branch of the axially symmetric spot mode under conditions of the third variant. The long-dashed lines represent mode 3 under conditions of the fourth variant.

There is good agreement between the modelling and the experiment on the spot mode. According to the modelling, protrusions cause reductions of the global tip temperature and the power losses, and these reductions are comparable to those measured in the super spot mode provided that the protrusion is elongated. Thus, the super spot mode observed in the work [6] may be explained as mode 3 of this work attached to an elongated protrusion.

After an arc operating in the super spot mode in the experiments [6] was turned off and then reignited, the super spot mode did not immediately re-appear and the spot mode was always observed. (In some cases, the spot mode changed into the super spot mode some time after the reignition. In other cases, the spot mode changed into the diffuse mode, i.e. the super spot mode did not re-appear at all.) The fact that the super spot mode does not re-appear immediately after the reignition of the arc could be understood if there were a special mechanism relating the super spot mode to molten tungsten [6], for example, if the electron emission increased when the emitted surface is molten. An alternative explanation may be suggested on the basis of simulation results shown in figure 11. The shape of a protrusion is governed by a balance of a number of forces, including surface tension, gravity, aerodynamic drag and the electromagnetic force. When the current is switched off, the aerodynamic drag and the electromagnetic force, which

maintain protrusions elongated, disappear, but surface tension and gravity persist and the protrusions assume a more or less spherical shape (seen in figure 8(d) of [6]) before the solidification. After the arc has been reignited, elongated protrusions must be formed once again before the super spot mode could re-appear.

Data on CVCs of cathodes operating in the spot and super spot modes taken from figure 15 of [6] are shown in figure 11(*c*). Also shown are modelling data obtained in the same way as above. Calculated values of the near-cathode voltage drop exceed values measured in the spot mode by about 30% and values measured in the super spot mode by about a factor of 2. This deviation is not surprising: the experimental values were derived from the cathode heat losses, and this procedure, while being acceptable in the case of the diffuse mode, becomes problematic in the case of the spot mode. The latter was discussed in section 3.4.3 of [9] and is also clear from the modelling data shown in figure 11: while thermal characteristics of the diffuse mode, spot mode and mode 3 are very different, the CVCs are not; in other words, variations of U and P_{L} are unrelated. The reason is that the reduction in total power losses of the cathode in the spot mode and mode 3 occurs not due to a reduced power input into the near-cathode plasma layer, but rather due to an increased power transported by the electron current from the near-cathode layer into the plasma bulk.

4.2. *High-current arcs*

Different modes of current transfer to cathodes of high-current arcs have received considerably less attention than those in low-current arcs. Rather detailed data on atmospheric-pressure argon arc at I =20–200 A have been reported in [7]. The cathode was made of (pure) tungsten in the form of a rod of 1 mm radius and 14–15 mm length. The cathode was pressed into a water-cooled copper holder to a depth of 5 mm, so the part of the cathode that was sticking out (i.e. was in contact with the plasma or the cold gas) had a length of 9–10 mm. Two forms of arc attachment to the cathode were observed, the diffuse mode and the constricted mode. The former is favoured by higher values of the stick-out length and the latter by lower values; the above-mentioned value of 9–10 mm was selected empirically so as to make the probabilities of the two modes comparable. If the arc was initiated at $I \lesssim 100$ A, either form of attachment may set in and persist for long, until a spontaneous switching to the other happens. At $I \approx 120$ A, a regular switching with a frequency of around 0.5 Hz was observed repeatedly. At $I \gtrsim 120$ A, the attachment of the arc was, as a rule, diffuse. If the arc attachment to the fresh cathode switched to the diffuse mode at $I \gtrsim 60$ A, the shape of the cathode tip changed and became hemispherical. At $I = 60$ A, this change took several tens of minutes. Data on axial distributions of the cathode surface temperature measured at three values of I on a cathode operating in the diffuse mode, taken from figure 6 of [7], are shown in figure 12. (z is the distance measured along the cathode axis from the tip in the direction inside the cathode body.)

Also shown in figure 12 are modelling results. Modelling of heat propagation inside the holder, although feasible, is

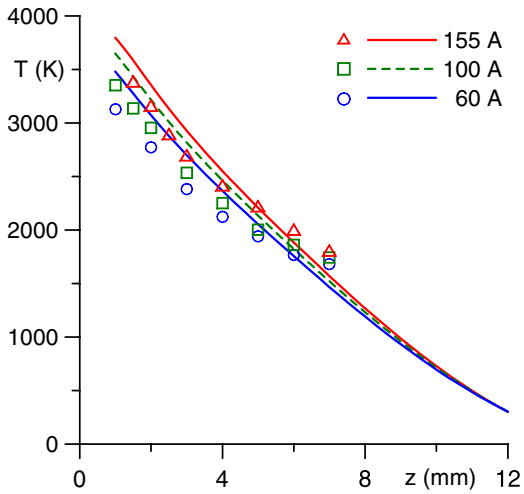

Figure 12. Axial distributions of the surface temperature of a 1 mm radius rod cathode at arc currents of 50, 100 and 155 A. Lines: modelling, mode 3. Points: experiment [7], diffuse mode.

hardly advisable at the present stage and the modelling was performed along the same lines as above. Three variants have been treated: a rod cathode of a height of 12 mm with a hemispherical tip; a rod cathode of a height of 12 mm with a flat tip; and a rod cathode of a height of 10 mm with a hemispherical tip. In terms of parameters specified in the beginning of section 3, these variants may be described as, respectively, $h = 12$ mm, $d = 1$ mm; $h = 12$ mm, $d = 0$; and $h = 10$ mm, $d = 1$ mm, with $R = 1$ mm and $R_p = 0$ in all variants. The cooling temperature T_{c} was set equal to 300 K.

In the first variant, mode 3 with a Z-shape localized in the current range 7.8 A $\lesssim I \lesssim$ 12.5 A was found. Two separate modes were found in the second variant, the diffuse mode and a 3D spot mode with a spot at the edge localized in the range $I \lesssim 34.3$ A. Mode 3 without a Z-shape was found in the third variant. Thus, only one mode of current transfer was found in each variant for the current values to which data in figure 12 refer, and this is the diffuse mode or the high-current section of mode 3 which comprises states typical for the diffuse mode.

It is known that characteristics of the diffuse mode are only weakly sensitive to variations of control parameters. Indeed, characteristics of the diffuse mode and mode 3 in the different above-described variants are rather close. For example, the near-cathode voltage at $I = 100$ A was 10.3 V, 10.3 V, 10.6 V in the first, second and third variants, respectively, while the temperature of the cathode surface at $z = 1$ mm was 3647, 3486 and 3598 K. For definiteness, we indicate that the lines in figure 12 represent modelling data under conditions of the first variant. According to both the experiment and the modelling, dependence of the temperature of the cathode surface on arc current is relatively weak, and the quantitative agreement is reasonable.

As far as the spot, or constricted, mode is concerned, the modelling correctly describes trends observed in the experiment, for example, the possible occurrence of both diffuse and spot modes at low currents and occurrence of only diffuse mode at currents high enough or the fact that the diffuse mode is favoured by higher values of the stick-out

length and the constricted mode by lower values. Another example is the observation that a stable axially symmetric attachment occurred only after the end of the rod had become hemispherical, which conforms to the modelling of this work. However, the range of existence of the spot mode in the experiment, which is up to 100 or 120 A, is considerably wider than the range in which two modes are obtained in the modelling, which is up to 12.5 A in the first above-described variant and 34.3 A in the second. Further work is clearly required, and this work should involve planning of experiments with account of modelling results.

4.3. Possibilities to be explored in future experiments

One of the results of the present modelling is the possibility of transition from the pattern with disconnected and stable diffuse and spot modes to a pattern with only one stable mode in a wide current range, which combines features of spot and diffuse modes. In situations where the first pattern occurs, the transition between the diffuse and spot modes is non-stationary and accompanied by hysteresis. Note that from the experimental point of view this situation includes not only cases in which the diffuse and spot modes found in the modelling are exactly disconnected as shown in figure 2, but also cases in which mode 3 possesses a Z-shape, as is the case under conditions of figure 4(c) in the current range $I \gtrsim 3$ A. In situations where only one stable mode exists in a wide current range (the second pattern), the transition between the diffuse distributions of the cathode surface temperature and distributions with spots may be realized in a quasi-stationary way without hysteresis. Furthermore, a minimum of the dependence of the temperature of the hottest point of the cathode on the arc current occurs during this quasi-stationary transition.

These conclusions may be verified experimentally in a relatively straightforward way. The experiment must be performed in a wide current range, including the range from 5 to 50 A, which is usually not covered, and be well controlled, since the sensitivity of the pattern on control parameters is in some cases very high. Cathodes with hemispherical or blunt conical tips may be used, provided that their dimensions and cooling system are suitably chosen. The minimum in the temperature of the hottest point of the cathode can cause similar minima in parameters of the near-cathode plasma and may be traced in this way.

Another conclusion that may be verified experimentally is the one on existence of stable regimes of current transfer which are intermediate between those characteristic for arc and glow cathodes and are associated with currents of several hundred milliamperes and nearcathode voltages of several hundred volts.

5. Conclusions

Variations of control parameters may dramatically change the pattern of steady-state modes of current transfer to a thermionic arc cathode. Three scenarios of these changes have been found: movement of the point of change of stability along a mode; bifurcation of modes of the same symmetry occurring at a certain combination of control parameters and accompanied by exchange of branches of the modes; junction of modes of the same symmetry which enters the considered range of arc currents from the region of very low currents.

The first scenario is at the origin of the change in stability of the high-temperature branch of the first axially symmetric spot mode which occurs in a transition from a cathode with the flat front surface to a cathode with the hemispherical front surface. The second or third scenarios are provoked by an increase in the curvature of the front surface of the cathode or in the cathode radius or by a decrease in the cathode height or the cooling temperature or by a protrusion on the front surface of the cathode. These scenarios result in a transition from the pattern with disconnected and stable diffuse and axially symmetric spot modes to a pattern with only one stable mode (mode 3) in a wide current range, which combines features of spot and diffuse modes at low and, respectively, high currents.

A pattern with two distinct modes may be viewed as a manifestation of self-organization, while a pattern with one mode is governed by a non-uniformity of the current-collecting surface of the cathode. On the other hand, all the above-mentioned variations of control parameters contribute to the diffuse mode becoming less uniform along the front surface. Therefore, the second and third above-described scenarios may be interpreted as a disappearance of self-organization due to an increasing non-uniformity of the current-collecting surface.

Modelling results provide an explanation for some observations made in experiments with low-current arcs typical for high-intensity discharge lamps. In particular, the super spot mode observed in the work [6] may be explained as mode 3 of this work attached to an elongated protrusion. There is also reasonable agreement between the modelling and the experiment [7] on cathodes operating in the diffuse mode at high arc currents. The modelling correctly describes trends observed in the experiment on spot mode in high-current arcs, however, the range of existence of the spot mode in the experiment exceeds that in the modelling. A further work is required, and this work should involve planning of experiments with account of modelling results.

The conclusions on existence under certain conditions of only one stable mode in a wide current range, which combines features of both spot and diffuse modes, and of a minimum of the dependence of the temperature of the hottest point of the cathode on the arc current, manifested by this mode, may have industrial importance and admit a relatively straightforward experimental verification.

Acknowledgments

The work was performed within the framework of the project PTDC/FIS/68609/2006, *Cathode spots in high-pressure dc gas discharges: self-organization phenomena* of FCT and FEDER and of the project *Centro de Ciências Matemáticas* of FCT, POCTI-219 and FEDER. M J Faria appreciates financial support from FCT through grant SFRH/BD/35883/2007.

References

[1] Thouret W, Weizel W and Günther P 1951 *Z. Physik* **130** 621–31
[2] Olsen H N 1963 *J. Quant. Spectrosc. Radiat. Transfer* **3** 305–33
[3] Haidar J 1995 *J. Phys. D: Appl. Phys.* **28** 2494–504
[4] Reiche J, Könemann F, Mende W and Kock M 2001 *J. Phys. D: Appl. Phys.* **34** 3177–84
[5] Lichtenberg S, Nandelstädt D, Dabringhausen L, Redwitz M, Luhmann J and Mentel J 2002 *J. Phys. D: Appl. Phys.* **35** 1648–56
[6] Hartmann T, Günther K, Lichtenberg S, Nandelstädt D, Dabringhausen L, Redwitz M and Mentel J 2002 *J. Phys. D: Appl. Phys.* **35** 1657–67
[7] Mitrofanov N K and Shkol'nik S M 2007 *Tech. Phys.* **52** 711–20
[8] Kühn G and Kock M 2007 *Phys. Rev.* E **75** 016406
[9] Benilov M S 2008 *J. Phys. D: Appl. Phys.* **41** 144001
[10] Almeida N A, Benilov M S and Naidis G V 2008 *J. Phys. D: Appl. Phys.* **41** 245201
[11] Könemann F, Kühn G, Reiche J and Kock M 2004 *J. Phys. D: Appl. Phys.* **37** 171–9
[12] Redwitz M, Dabringhausen L, Lichtenberg S, Langenscheidt O, Heberlein J and Mentel J 2006 *J. Phys. D: Appl. Phys.* **39** 2160–79
[13] Bade W L and Yos J M 1963 *Theoretical and Experimental Investigation of Arc Plasma-Generation Technology. Part II, vol. 1: A Theoretical and Experimental Study of Thermionic Arc Cathodes. Technical Report No ASD-TDR-62-729* (Wilmington, MA, USA: Avco Corporation)
[14] http://www.arc_cathode.uma.pt
[15] Benilov M S 1998 *Phys. Rev.* E **58** 6480–94
[16] Benilov M S and Cunha M D 2003 *J. Phys. D: Appl. Phys.* **36** 603–14
[17] Benilov M S, Carpaij M and Cunha M D 2006 *J. Phys. D: Appl. Phys.* **39** 2124–34
[18] Dabringhausen L, Langenscheidt O, Lichtenberg S, Redwitz M and Mentel J 2005 *J. Phys. D: Appl. Phys.* **38** 3128–42
[19] Scharf F H, Langenscheidt O and Mentel J 2007 *Proc. 28th ICPIG (Prague, July 2007)* ed J Schmidt *et al* (Prague: Institute of Plasma Physics AS CR) ISBN 978-80-87026-01-4, pp 1252–5
[20] Bötticher R and Bötticher W 2000 *J. Phys. D: Appl. Phys.* **33** 367–74
[21] Benilov M S 2007 *J. Phys. D: Appl. Phys.* **40** 1376–93
[22] Benilov M S and Faria M J 2007 *J. Phys. D: Appl. Phys.* **40** 5083–97
[23] Benilov M S, Cunha M D and Faria M J 2008 *IEEE Trans. Plasma Sci.* **36** 1034–5
[24] Dabringhausen L, Hechtfischer U, Vos T, van Erk W and Haacke M 2007 *Proc. 11th Int. Sympon. Science and Technology of Light Sources (LS:11, Shanghai, China, May 2007)* ed M Q Liu and R Devonshire (Sheffield, UK: FAST-LS) ISBN 978-0-9555445-0-7, pp 285–6
[25] Rahmane M, Croquesel E and Selezneva S 2007 High pressure discharge lamp control system and method *United States Patent* US 7250732 B2
[26] Li H P, Chazelas C, Wu G Q, Benilova L G, Wang H X, Benilov M S, Mariaux G and Vardelle A 2009 *Proc. 19th Int. Symp. on Plasma Chemistry (Bochum, Germany, 26–31 July 2009)* (Bochum: Ruhr-Universität Bochum)
[27] Benilov M S, Cunha M D and Naidis G V 2005 *Plasma Sources Sci. Technol.* **14** 517–24
[28] Benilov M S, Jacobsson S, Kaddani A and Zahrai S 2001 *J. Phys. D: Appl. Phys.* **34** 1993–9
[29] Benilov M S and Faria M J 2008 *Proc. European COMSOL Conf. (Hannover, Germany 4–6 November 2008)* http://cds.comsol.com/access/dl/papers/5322/Faria.pdf
[30] Touloukian Y S, Powell R W, Ho C Y and Clemens P G 1970 *Thermal Conductivity. Metallic Elements and Alloys* (*Thermophysical Properties of Matter*) vol 1 (New York-Washington: IFI/Plenum)
[31] Yih S W H and Wang C T 1979 *Tungsten: Sources, Metallurgy, Properties, and Applications* (New York: Plenum)
[32] Almeida P G C, Benilov M S, Cunha M D and Faria M J 2009 *J. Phys. D: Appl. Phys.* **42** at press (Cluster Issue on Plasma Modelling)
[33] Mentel J, Luhmann J and Nandelstädt D 2000 *Industry Applications Conf. 2000 (Rome, Italy) Conf. Record of the 2000 IEEE* vol 5 3293–300
[34] Luijks G M J F, Nijdam S and v Esveld H 2005 *J. Phys. D: Appl. Phys.* **38** 3163–9
[35] Schoenbach K H, Moselhy M and Shi W 2004 *Plasma Sources Sci. Technol.* **13** 177–85
[36] Yang Y, Shi J J, Harry J E, Proctor J, Garner C P and Kong M G 2005 *IEEE Trans. Plasma Sci.* **33** 302–3
[37] Staack D, Farouk B, Gutsol A and Fridman A 2008 *Plasma Sources Sci. Technol.* **17** 025013